DE GRUYTER Z. Naturforsch. 2018; 73(11)b: 753–758

Enrique J. Baran*, Oscar E. Piro, Gustavo A. Echeverría and Beatriz S. Parajón-Costa

Structural and IR-spectroscopic characterization of pyridinium acesulfamate, a monoclinic twin

https://doi.org/10.1515/znb-2018-0074
Received April 24, 2018; accepted July 18, 2018

Abstract: The crystal structure of pyridinium 6-methyl-1,2,3,-oxathiazine-4(3*H*)-one-2,2-dioxide [(C_5NH_6)($C_4H_4NO_4S$)], for short, pyH(ace), was determined by X-ray diffraction methods. It crystallizes as a twin in the monoclinic space group $P2_1/c$ with $a=6.9878(9)$, $b=7.2211(7)$, $c=21.740(2)$ Å, $\beta=91.67(1)°$ and $Z=4$ molecules per unit cell. The structure was determined employing 1599 reflections with $I>2\sigma(I)$ from one of the twin domains and refined employing 2092 reflections from both crystal domains to an agreement R1 factor of 0.0466. Besides electrostatic attractions, intermolecular pyH···O=C(ace) hydrogen bonds stabilize the acesulfamate anion and the pyridinium cation into planar discrete units parallel to the (100) crystal plane. The units form stacks of alternating ace$^-$ and pyH$^+$ ions along the *a* axis that favors inter-ring π–π interactions. The Fourier transform-infrared (FT-IR) spectrum of the compound was recorded and is briefly discussed. Some comparisons with related pyridinium saccharinate salts are also made.

Keywords: crystal structure; FT-IR spectrum; pyridinium acesulfamate; synthesis.

Dedicated to: Professor Bernt Krebs on the occasion of his 80th birthday.

1 Introduction

Acesulfame-K, the potassium salt of 6-methyl-1,2,3-oxathiazin-4(3*H*)-one-2,2-dioxide, is one of the most widely used low-calorie artificial sweeteners [1, 2], and its general chemical and biological properties have been thoroughly investigated [1–3].

From the chemical and structural points of view, the acesulfamate anion bears some resemblance to saccharin (1,2-benzothiazole-3(2*H*)-one-1,1-dioxide) (Fig. 1), whose coordination capacity has been intensively explored during the last years (for a recent review, *cf.* [4]). Different studies have exploited these analogies, and an important number of metal complexes containing the acesulfamate anion as a ligand have also been reported (*cf.* for example [5] and references therein). Also, a great number of simple salts of this anion have recently been characterized [6–14].

During the last years, a number of interesting supramolecular structures of co-crystals containing saccharin and different organic bases have been prepared and characterized [15–20], studies that we have also extended to systems containing thiosaccharin instead of saccharin [21–23].

Taking into account the structural and chemical analogies between saccharin and acesulfamic acid, it seems now interesting to investigate the possible formation of such type of co-crystals based on the latter acid. In this paper, we report the first example of such a system, obtained by the interaction of acesulfamic acid and pyridine.

2 Results and discussion

Pyridinium acesulfamate, pyH(ace), was obtained by dissolution of acesulfamic acid in pyridine, as described in the Experimental section. It crystallizes in the monoclinic space group $P2_1/c$ with $Z=4$ formula units.

An Ortep [24] plot of the pyH(ace) salt is shown in Fig. 2 and corresponding bond lengths and angles are given in Table 1. The metrics for the acesulfamate part are in accordance with the corresponding values reported for the closely related ammonium acesulfamate [8] and other related salts, including the family of acesulfamates of the alkali metals, namely, *M*(ace) with *M* = Li, Na, K, Rb, Cs, where the heavier metal members (*M* = Na to Cs) constitute an isomorphic series [6, 9, 14]. Particularly, the short C3–C4 distance of 1.309(3) Å confirms the formal double

***Corresponding author: Enrique J. Baran,** Facultad de Ciencias Exactas, Centro de Química Inorgánica (CEQUINOR/CONICET-CCT-La Plata, UNLP), Universidad Nacional de La Plata, Bvd. 120, No. 1465, 1900-La Plata, Argentina, e-mail: baran@quimica.unlp.edu.ar
Oscar E. Piro and Gustavo A. Echeverría: Facultad de Ciencias Exactas, Departamento de Física and Instituto IFLP (CONICET-CCT-La Plata), Universidad Nacional de La Plata, 1900-La Plata, Argentina
Beatriz S. Parajón-Costa: Facultad de Ciencias Exactas, Centro de Química Inorgánica (CEQUINOR/CONICET-CCT-La Plata, UNLP), Universidad Nacional de La Plata, Bvd. 120, No. 1465, 1900-La Plata, Argentina

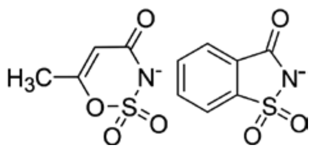

Fig. 1: Schematic drawings of the structure of acesulfamate (left) and saccharinate (right) anions.

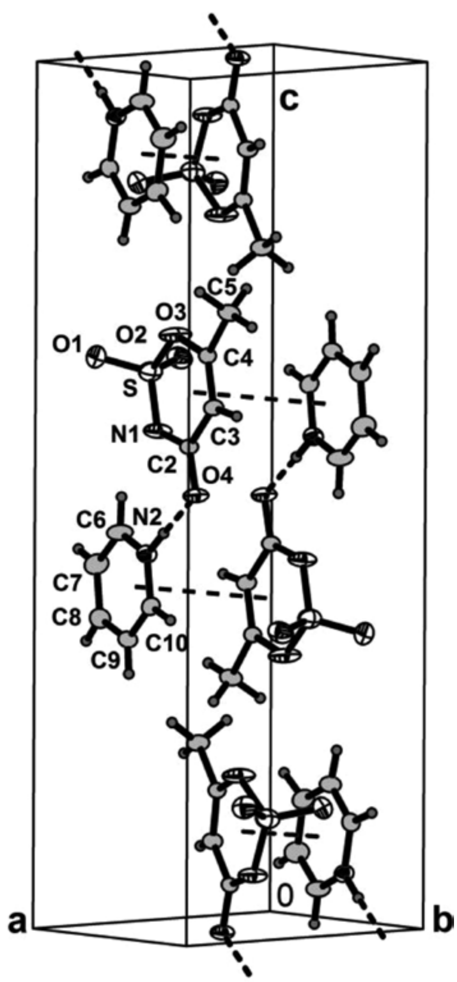

Fig. 2: View of the pyrH(ace) salt showing the labeling of the non-H atoms and their displacement ellipsoids at the 30% probability level. Hydrogen bonds and π–π interactions are indicated by dashed lines. The pyrH(ace) unit next to the labeled one is obtained through the inversion symmetry operation 1 – *x*, 1 – *y*, 1 – *z*.

bond character expected for this link. The carbonyl >C=O double bond length is 1.251(2) Å and the sulfoxide S=O bond lengths are 1.405(2) and 1.410(2) Å. The other ring single bond lengths are d(C–O) = 1.354(3) Å, d(O–S) = 1.622(2) Å, d(S–N) = 1.544(2) Å, d(C–N) = 1.327(3) Å and d(C–C) = 1.437(3) Å. These bond lengths can be compared with those in the solid state of the neutral acesulfamic acid. It crystallizes in two polymorphic forms, one in the triclinic space group $P\overline{1}$ with $Z = 2$ molecules per unit cell and the other one in the monoclinic space group $P2_1/c$ with two different molecules per asymmetric unit ($Z = 8$) [25]. Referring to the better refined triclinic form, the major change in the bonding in the structure of the acesulfamate ion in the pyH(ace) salt occurs at the S–N bond, which, upon deprotonation, shortens by 0.085 Å (about 30 times the standard error σ). A smaller shortening (–0.055 Å = –14 σ) is observed in the N–C bond length.

Table 1: Bond lengths (Å) and angles (deg) of pyridinium acesulfamate.

C(2)–O(4)	1.251(2)	C(1)–C(2)–C(3)	119.5(2)
C(2)–N(1)	1.327(3)	C(4)–C(3)–C(2)	125.2(3)
C(2)–C(3)	1.437(3)	C(3)–C(4)–O(3)	120.7(2)
C(3)–C(4)	1.309(3)	C(3)–C(4)–C(5)	128.5(3)
C(4)–O(3)	1.354(3)	O(3)–C(4)–C(5)	110.7(2)
C(4)–C(5)	1.485(4)	N(2)–C(6)–C(7)	120.5(3)
C(6)–N(2)	1.327(3)	C(8)–C(7)–C(6)	119.1(3)
C(6)–C(7)	1.360(4)	C(9)–C(8)–C(7)	119.3(3)
C(7)–C(8)	1.364(4)	C(8)–C(9)–C(10)	119.9(3)
C(8)–C(9)	1.365(4)	N(2)–C(10)–C(9)	119.8(3)
C(9)–C(10)	1.358(4)	C(2)–N(1)–S	123.4(2)
C(10)–N(2)	1.323(3)	C(6)–N(2)–C(10)	121.6(3)
N(1)–S	1.544(2)	C(4)–O(3)–S	121.5(2)
O(1)–S	1.410(2)	O(2)–S–O(1)	115.6(1)
O(2)–S	1.405(2)	O(2)–S–N(1)	112.7(2)
O(3)–S	1.622(2)	O(1)–S–N(1)	111.8(2)
O(4)–C(2)–N(1)	119.6(2)	O(2)–S–O(3)	104.8(2)
O(4)–C(2)–C(3)	120.9(2)	O(1)–S–O(3)	102.8(2)
		N(1)–S–O(3)	108.2(1)

In the pyridinium ion, C–C bond lengths are in the range 1.358(4)–1.365(4) Å and C–N bond lengths are 1.323(3) and 1.327(3) Å, as expected for a heteroarene structure.

The pyridinium acesulfamate salt is arranged in the lattice as discrete bimolecular units that, besides electrostatic attraction, are stabilized by a strong and linear (py)NH···O=C(ace) hydrogen bond [d(H···O) = 1.77(3) Å, ∠(N–H···O) = 178(3)°], nearly directed along one oxygen electron lone pair lobe. Acesulfamate and pryridinium ions lie nearly on the same non-crystallographic mirror plane (*rms* deviation of atoms from the best least-squares plane of 0.041 Å) and are arranged in the lattice as a layered structure parallel to the crystal (100) plane. This is not accidental as it turns out that the monoclinic space group $P2_1/c$ (#14) crystal can be achieved for pyH(ace) (after a cyclic unit cell axes transformation) through a slight distortion of the orthorhombic super-group *Pnma* (#62), where the molecular ions lie on a crystallographic *m* (mirror) plane. The slight departure of the acesulfamate molecule from strict planarity is the origin of the symmetry breaking transforming the space group symmetry from *Pnma* into its subgroup $P2_1/c$.

Neighboring pyH(ace) units are related through crystallographic inversion centers and piled up along the crystallographic *a* axis (see Fig. 2). The partially eclipsed ace^- and pyH^+ rings alternate along the stacks at a distance of about 3.45 Å (≈*a*/2) from each other. Besides electric dipole–dipole and van der Waals attractions, the stacking is thus stabilized by ring π–π interactions.

The molecular packing is further stabilized by weak interactions, including a long and bent intra-bimolecular N–H···O bond and also inter-bimolecular C–H···O and C–H···N links. The hydrogen bond parameters are detailed in Table 2. The packing of the components shows that the ion pairs are not bonded any further along the crystallographic *c* axis, an observation that could explain why (001) is both an easy-cleavage and twinning crystal plane.

Curiously, ammonium and acesulfamate ions present a similar association in the (NH_4)(ace) salt, which also shows a crystal packing closely related to pyH(ace). In fact, the ammonium salt crystallizes in the space group *Pnma* with $a=9.5047(6)$ Å, $b=6.9273(6)$ Å, $c=11.5255(6)$ Å and $Z=4$. Here, the bimolecular (NH_4)(ace) units lie on a crystallographic mirror plane with the acesulfamate anion showing positional disorder at the ring oxygen atom, which was adequately modeled in terms of two split mirror-related positions [8]. The similar packing of pyH(ace) and (NH_4)(ace) salts explains the almost equal values in the observed lengths of their respective *a* [= 6.9878(9) Å] and *b* [= 6.9273(6) Å] cell constants as they are both equal to twice the stacking distance (of about 3.45 Å).

The monoclinic (quasi-orthorhombic) crystal structure of pyH(ace) can also be compared with the related pyridinium saccharinate, pyH(sac), salt. Despite crystallizing in the lower-symmetric space group $P\bar{1}$ with two

Table 2: Hydrogen bond lengths (Å) and angles (deg) for pyridinium acesulfamate.[a]

D–H···A	d(D–H)	d(H···A)	d(D···A)	∠(D–H···A)
N(2)–H(2N)···N(1)	0.92(3)	2.57(2)	3.173(3)	123(2)
N(2)–H(2N)···O(4)	0.92(3)	1.77(3)	2.693(3)	178(3)
C(5)–(5A))···O(1)#1	0.99(4)	2.58(4)	3.539(5)	163(3)
C(5)–(5B)···O(2)#2	0.92(3)	2.61(3)	3.486(5)	160(3)
C(6)–H(6)···N(1)	0.89(3)	2.57(3)	3.210(4)	130(2)
C(7)–H(7)···O(4)#3	0.91(3)	2.54(3)	3.401(4)	160(2)

[a]Symmetry transformations used to generate equivalent atoms: (#1) $-x+2$, $y+1/2$, $-z+3/2$; (#2) $-x+1$, $y+1/2$, $-z+3/2$; (#3) x, $y-1$, z.

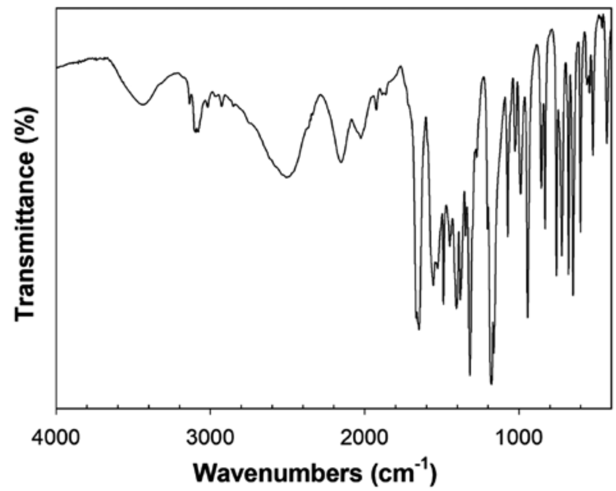

Fig. 3: FT-IR spectrum of pyridinium acesulfamate in the spectral range between 4000 and 400 cm^{-1}.

independent molecules per asymmetric unit ($Z=4$), it also shows almost planar discrete pyH(sac) assemblies, linked through intermolecular pyH···O=C(sac) bonds. As for pyH(ace), the pyH(sac) units form stacks throughout the lattice, where sac^- and pyH^+ ions alternate along the stacks at distances in the 3.7–4.0 Å range. This arrangement indicates that the stacks are further stabilized by inter-ring π–π interactions [20].

The Fourier transform-infrared (FT-IR) spectrum of the salt is relatively complex, presenting an important number of bands, as shown in Fig. 3, and as expected for the simultaneous presence of acesulfamate and pyridinium vibrations. The assignment of the acesulfamate vibrations was made on the basis of an experimental and theoretical study of potassium acesulfamate [26], as well as on the information compiled in our previous spectroscopic studies of this anion [8–10, 12–14]. Vibrations of the pyridinium cation were analyzed with the aid of a series of classic [27–33] and most recent [34, 35] papers on this ion, as well as on free pyridine. The proposed assignments are shown in Table 3 and are briefly discussed as follows:

- Pyridinium salts, pyH^+/A^-, represent a class of complexes with inter-ionic hydrogen bonds. It is well known that the ν(N–H) stretching bands in the infrared spectra of these salts present relatively complex shapes [30–33]. It is also admitted that the important band shape distortions is due to Fermi resonance effects, originating from the vibrational coupling between the ν(N–H) fundamental and internal modes of the pyridinium ion [33].
- In the present case, the ν(N– H) vibration appears as three relatively strong and broad bands located at 2507, 2153 and 2025 cm^{-1}. In the case of the related

Table 3: Assignment of the FT-IR spectrum of pyridinium acesulfamate.[a]

IR bands (positions in cm^{-1})	Assignment
3135 w, 3094 m, 3012 w, 2927 w	ν(C–H)
2507 s, br, 2153 s, br, 2025 m, br	ν(N–H) (pyH^+)
1925 w, 1884 vw, 1864 vw	Overtones py-ring (*cf*. text)
1666 sh, 1648 vs	ν(C=O)+ν(C–C)$_{ring}$ (ace)
1555 vs, br, 1527 m	$\nu_{ring}+\delta$(CH) (py)
1489 s, 1449 m, 1441 sh	$\nu_{ring}+\delta$(CH) (py)
1405 s, 1400 sh	$\delta(CH_3)$ (ace) + δ(NH) (pyH^+)
1380 s	$\nu_{as}(SO_2)$ (ace)
1345 m	$\nu_{ring}+\delta$(CH) (py)
1317 vs, 1284 sh	ν(CN)+ν(OC)+δ(CCH) (ace)
1273 w	$\nu_{ring}+\delta$(CH) (py)
1204 w, 1177 vs	$\nu_s(SO_2)+\nu$(SN) (ace)
1164 m	$\nu_{ring}+\delta$(CH) (py)
1073 s	$\delta(CH_3)$ (ace) + $\nu_{ring}+\delta$(CH) (py)
1054 sh	$\nu_{ring}+\delta$(CH) (py)
1027 m, 1021 sh	ν_{ring} (py) + ν(OC)+ν(SN) (ace)
989 s	ν_{ring} (py) + γ(NH) (pyH^+)
944 vs	ν(OC)+$\nu(C–CH_3)$ (ace) + γ(CH) (py)
855 s	τ_{ring} (ace)
831 vs	ν(SN)+ν(CC)+δ(NCO) (ace)
757 vs, 722 vs	τ_{ring} (ace) + γ(CH)+τ_{ring} (py)
678 vs	δ_{ring} (ace)
649 vs, 601 vs	ν_{ring} (py)
561 m, 553 m, 543 m	$\tau_{ring}+\delta_{ring}+\delta(SO_2)$ (ace)
520 s, 473 sh, 461 w, 430 s	δ_{ring} (ace)

[a]vs, very strong; s, strong; m, medium; w, weak, vw, very weak; br, broad; sh, shoulder.

pyridinium saccharinate, pyH(Sac), a similar spectral band pattern is observed for this vibration, with the three bands at 2456, 2157 and 2044 cm^{-1}.

– The following weak bands correspond to the characteristic series of three overtone vibrations, which in liquid pyridine were found at 1987, 1923 and 1872 cm^{-1} [28] (*cf.* also [36]). These bands are, essentially, binary combinations and/or overtones of aryl wagging motions [37, 38].
– The analysis of the pyridinium ν(C–H) motions, as well as the ring stretching and bendings, shows a close correspondence with the vibrations reported for free pyridine, although with small band displacements to lower or higher energies in the different spectral ranges. CH bending vibrations in the 1600–1000 cm^{-1} range can be assigned to in-plane deformations and are usually strongly coupled with ring motions; bending vibrations below 1000 cm^{-1} are generally related to out-of-plane vibrations [38]. It was very difficult to assign the N–H bending vibrations. These vibrations are strongly coupled with ring motions, and their positions also depend on the characteristics of the counterion present in the crystal structure [30, 32, 35]. Therefore, our assignments of 989 cm^{-1} to the γ(NH) mode and of the 1405/1400 cm^{-1} feature to the δ(NH) mode may be considered as tentative only.
– Some bands of the acesulfamate ion also show minor changes after the formation of the pyridinium salt. For example, the typical doublet structure in the region about 1600 cm^{-1}, found in all simple acesulfamate salts [8–10, 12–14] and assigned to the ν(C=O)+ν(C–C)$_{ring}$ vibrations, appears in the present case as a unique band with a weak shoulder at its higher energy side. On the other hand, the $\nu_{as}(SO_2)$ vibration suffers a small blue-shift in comparison with the values found, for example, in the alkaline-metal acesulfamates [9, 14], whereas the position of the corresponding symmetric mode remains unchanged.
– Finally, it must be commented that the relatively broad band seen at the highest energy (3437 cm^{-1}) in Fig. 3 is due to a small quantity of absorbed humidity in our measurement device, which was very difficult to remove.

In the case of pyridinium saccharinate, the pyH^+ bands also occur practically in the same energy ranges as in the acesulfamate salt. In this case, we have tentatively assigned the δ(NH) and γ(NH) modes to two weak signals found at 1413 and 1019 cm^{-1}, respectively. Interestingly, the above-mentioned typical triplet overtone structure is seen in this case as a single, weak and slightly deformed band centered at 1865 cm^{-1}. Most of the saccharinate bands are also slightly displaced to higher or lower frequencies in this salt, in comparison with the values reported, for example, in sodium saccharinate [39, 40], and also here, the $\nu_{as}(SO_2)$ vibration is also blue-shifted, whereas $\nu_s(SO_2)$ remains at the same frequency as in the sodium salt.

3 Experimental section

3.1 Materials and measurements

Potassium acesulfamate was supplied by Fluka (Sigma-Aldrich, Steinheim, Germany), and saccharin was supplied by ALDRICH (St. Louis, MO, USA). All the other reagents were from Merck (Darmstadt, Germany), were of analytical grade, and were used as purchased. Elemental analysis was performed with a Carlo Erba (Milano, Italy) model EA 1108 elemental analyzer. The infrared absorption spectra were recorded on a FT-IR Bruker-EQUINOX 55 spectrophotometer (Bruker Optics Inc., Billerica, MA, USA), in the range between 4000 and 400 cm^{-1}, using the KBr pellet technique.

3.2 Syntheses of the compounds

Acesulfamic acid was prepared as described by Velaga et al. [25], as follows: To 5.00 g of potassium acesulfamate dissolved in a small portion of water (*ca.* 10 mL), 6 mL of concentrated HCl was added drop-wise. The generated acid was extracted with 20 mL of ethyl acetate. After evaporation of the solvent in air, a colorless solid was deposited. It was recrystallized twice from ethyl acetate, generating a deposit of needle-like colorless crystals, after slow evaporation of the solvent in air (m. p. 122–124°C [25]).

For the synthesis of the pyridinium acesulfamate, 2.0 mmol (0.32 g) of acesulfamic acid was dissolved in 15 mL of pyridine under constant stirring. The mixture was further stirred for 30 min and then kept at room temperature for evaporation of the excess pyridine. After a few days, colorless crystals were obtained. Its purity was confirmed by elemental analysis: $C_9H_{10}N_2O_4S$ (242.25): calcd., C 44.58, H 4.13, N 11.56, S 13.23; found, C 44.55, H 4.17, N 11.50, S 13.20%. Single crystals adequate for X-ray diffraction studies were selected from the crystalline mass employing a microscope.

The related pyridinium saccharinate, synthesized for comparative purposes, was prepared in the same way, dissolving 2.0 mmol of saccharin in 20 mL of pyridine [20]: Elemental analysis: $C_{12}H_{10}N_2O_3S$ (262.28): C 54.90, H 3.81, N 10.67, S 12.22; found, C 54.85, H 3.85, N 10.60, S 12.15%.

3.3 X-ray structure determination

X-ray diffraction measurements were performed on an Oxford Xcalibur, Eos, Gemini CCD diffractometer employing graphite-monochromated MoKα radiation ($\lambda = 0.71073$ Å). Intensities were collected (ω scans with ϑ and κ-offsets), integrated and scaled with the CrysAlis Pro [41] suite of programs. The unit cell parameters were obtained by least-squares refinement (based on the angular settings for all collected reflections with intensities larger than seven times the standard deviation of measurement errors) using CrysAlis Pro. Data were corrected empirically for absorption employing the multiscan method implemented in CrysAlis Pro.

Most of the diffraction pattern was interpreted in terms of two monoclinic crystal domains (twins) related to each other through a rotation of 180° around the reciprocal c^* axis (almost coincident with the direct *c* axis). The unit cell parameters for both twins were equal within experimental accuracy. The reflections were indexed in the reciprocal unit cell of the corresponding domains. It was resorted to the twin crystal data reduction facility implemented in CrysAlis Pro to generate two data sets, namely, a regular one with the diffraction data indexed in the reciprocal unit cell of the largest domain (hereafter called twin #1) and a second one including all the reflections from both domains with the overlapping ones flagged for structure development and refinement.

The full data set for twin #1 (with about 62% of diffracting power) was employed to solve the structure by the intrinsic phasing procedure implemented in Shelxt [42] and the corresponding non-H molecular model refined with anisotropic displacement parameters with Shelxl [43]. Despite a correct molecular model, however, the refinement showed evidence of the presence of overlap between reflections from both crystal twins. This evidence included (besides the visual rendering of the weighted reciprocal space implemented in CrysAlis Pro) a relatively high *R*1 value for this stage ($R1 = 0.1040$) and the list

Table 4: Crystal data, X-ray diffraction data and refinement results for pyridinium acesulfamate.

Empirical formula	$C_9H_{10}N_2O_4S$
Formula weight	242.25
T, K	297(2)
Cryst. dimensions, mm^3	0.351 × 0.187 × 0.086
Cryst. shape and color	Colorless plate
Cryst. system	Monoclinic
Space group	$P2_1/c$
a, Å	6.9878(9)
b, Å	7.2211(7)
c, Å	21.740(2)
β, deg.	91.67(1)
Volume, $Å^3$	1096.5(2)
Z	4
Calculated density, g cm^{-3}	1.47
Absorption coefficient, mm^{-1}	0.3
F(000), *e*	504
θ range, data collection, deg.	2.973–29.009
Index ranges, *hkl*	±9 ±9 −28/+29
Reflections collected	4035
Independent reflections/R_{int}	4035/0.0641
Observed reflections [$I > 2\sigma(I)$]	2092
Refinement method	Full-matrix least-squares on F^2
Data/restraints/parameters	4035/0/186
$R1/wR2$ [$I > 2\sigma(I)$]	0.0466/0.0919
$R1/wR2$ (all data)	0.0978/0.1013
Goodness of fit on F^2	0.826
Largest peak/hole, *e* $Å^{-3}$	0.31/−0.40

of the most disagreeing reflections showing systematically larger *F*(obs) as compared with *F*(calcd) values. We therefore refined the initial molecular model against the second data set, which includes all collected reflections for both crystal domains, employing the untwining process implemented in Shelxl. Now, the *R*1 factor dropped to 0.0693, and the sign of the *F*(obs)–*F*(calcd) difference for the most disagreeing reflections was more evenly distributed. The ensuing difference Fourier map showed all the hydrogen atoms among the first 11 residual peaks. These atoms were refined at their found positions with isotropic displacement parameters. The methyl H atoms converged to a staggered conformation. The occupancy of domain #2 was 0.377(1). Because we are dealing with the diffraction data from two independent domains of the same solid, the observed data $[I > 2\sigma(I)]$ to parameter ratio increased from 8.54 to 11.25. Crystal data, data collection procedure and refinement results are summarized in Table 4.

CCDC 1834840 contains the supplementary crystallographic data for this paper. These data can be obtained free of charge from The Cambridge Crystallographic Data Centre *via* www.ccdc.cam.ac.uk/data_request/cif.

Acknowledgments: This work was supported by CONICET (PIP 11220130100651CO) and UNLP (Grants 11/X709 and 11/X673) of Argentina. OEP, GAE, and BSP-C are Research Fellows from CONICET.

References

[1] D. G. Mayer, F. H. Kemper (Eds.), *Acesulfame-K*, Marcel Dekker, New York, **1991**.
[2] M. A. Cantarelli, R. G. Pellerano, E. J. Marchevsky, J. M. Camiña, *Food Chem.* **2009**, *115*, 1128.
[3] K. Clauss, H. Jensen, *Angew. Chem. Int. Ed. Engl.* **1973**, *12*, 869.
[4] E. J. Baran, V. T. Yilmaz, *Coord. Chem. Rev.* **2006**, *250*, 1980.
[5] H. Içbudak, E. Adiyaman, A. Uyanik, S. Çakir, *Transit. Metal Chem.* **2007**, *32*, 864.
[6] E. F. Paulus, *Acta Crystallogr*. **1975**, *B31*, 1191.
[7] G. Demirtas, N. Dege, H. Icbudak, O. Yurdakul, O. Büyükgüngör, *J. Inorg. Organomet. Polym*. **2012**, *22*, 671.
[8] G. A. Echeverría, O. E. Piro, B. S. Parajón-Costa, E. J. Baran, *Z. Naturforsch.* **2014**, *69b*, 737.
[9] O. E. Piro, G. A. Echeverría, B. S. Parajón-Costa, E. J. Baran, *Z. Naturforsch.* **2015**, *70b*, 491.
[10] E. J. Baran, B. S. Parajón-Costa, G. A. Echeverría, O. E. Piro, *Maced. J. Chem. Chem. Eng.* **2015**, *34*, 95.
[11] H. Icbudak, G. Demirtas, N. Dege, *Maced. J. Chem. Chem. Eng.* **2015**, *34*, 105.
[12] O. E. Piro, G. A. Echeverría, B. S. Parajón-Costa, E. J. Baran, *Z. Naturforsch.* **2016**, *71b*, 51.
[13] G. A. Echeverría, O. E. Piro, B. S. Parajón-Costa, E. J. Baran, *Z. Naturforsch.* **2017**, *72b*, 739.
[14] O. E. Piro, G. A. Echeverría, B. S. Parajón-Costa, E. J. Baran, *J. Chem. Crystallogr.* **2017**, *47*, 226.
[15] Z. L. Wang, L. H. Wei, M. X. Li, J. Y. Niu, *Acta Crystallogr.* **2006**, *E62*, o1314.
[16] Z. L. Wang, L. H. Wei, M. X. Li, J. P. Wang, *Acta Crystallogr.* **2006**, *E62*, o1800.
[17] Z. L. Wang, M. X. Li, L. H. Wei, J. P. Wang, *Acta Crystallogr.* **2006**, *E62*, o2127.
[18] Z. L. Wang, M. X. Li, L. H. Wei, J. P. Wang, *Acta Crystallogr*. **2006**, *E62*, o2171.
[19] R. Banerjee, B. K. Saha, G. R. Desiraju, *Acta Crystallogr*. **2006**, *C62*, o346.
[20] Z. L. Wang, M. X. Li, L. H. Wei, J. P. Wang, *Acta Crystallogr.* **2006**, *E62*, o2274.
[21] E. J. Baran, O. E. Piro, J. Zinczuk, *Z. Naturforsch.* **2007**, *62b*, 1530.
[22] O. E. Piro, J. Zinczuk, E. J. Baran, *Z. Naturforsch.* **2008**, *63b*, 877.
[23] G. A. Echeverría, O. E. Piro, J. Zinczuk, E. J. Baran, *J. Argent. Chem. Soc.* **2017**, *104*, 1.
[24] L. J. Farrugia, *J. Appl. Crystallogr.* **1997**, *30*, 565.
[25] S. P. Velaga, V. R. Vangala, S. Basavoju, D. Boström, *Chem. Commun.* **2010**, *46*, 3562.
[26] A. D. Popova, E. A. Velcheva, B. A. Stamboliyska, *J. Mol. Struct.* **2012**, *1009*, 23.
[27] C. H. Kline, J. Turkevich, *J. Chem. Phys.* **1944**, *12*, 300.
[28] L. E. Corrsin, B. J. Fax, R. C. Lord, *J. Chem. Phys.* **1953**, *21*, 1170.
[29] N. S. Gill, R. H. Nuttall, D. E. Scaife, D. W. A. Sharp, *J. Inorg. Nucl. Chem.* **1961**, *18*, 79.
[30] D. E. Cook, *Can. J. Chem.* **1961**, *39*, 2009.
[31] S. E. Odinokov, A. A. Mashkovsky, V. P. Glazunov, A. V. Iogansen, B. V. Rassadin, *Spectrochim. Acta* **1976**, *32A*, 1355.
[32] V. P. Glazunov, S. E. Odinokov, *Spectrochim. Acta* **1982**, *38A*, 399.
[33] V. P. Glazunov, S. E. Odinokov, *Spectrochim. Acta* **1982**, *38A*, 409.
[34] F. Partal Ureña, M. Fernández Gómez, J. J. López González, E. Martínez Torres, *Spectrochim. Acta* **2003**, *59A*, 2815.
[35] B. A. Omidvar, S. F. Tayyari, M. Vakili, A-R. Nekoei, *Spectrochim. Acta* **2018**, *191A*, 558.
[36] B. Schrader, *Raman/Infrared Atlas of Organic Compounds*, 2nd ed., Verlag Chemie, Weinheim, **1989**.
[37] D. H. Whiffen, *Spectrochim. Acta* **1955**, *7*, 253.
[38] D. Lin-Vien, N. B. Colthup, W. G. Fateley, J. G. Grasselli, *Handbook of Infrared and Raman Characteristic Frequencies of Organic Molecules*, Academic Press, Boston, **1991**.
[39] O. V. Quinzani, S. Tarulli, O. E. Piro, E. J. Baran, E. E. Castellano, *Z. Naturforsch.* **1997**, *52b*, 183.
[40] A. Brizuela, E. Romano, A. Yurquina, S. Locatelli, S. A. Brandán, *Spectrochim. Acta* **2012**, *95A*, 399.
[41] CrysAlis Pro (version 1.171.33.48, release 15-09-2009, CrysAlis 171.NET), Oxford Diffraction Ltd. Abingdon, Oxford (UK) **2009**.
[42] G. M. Sheldrick, *Acta Crystallogr.* **2015**, *A71*, 3.
[43] G. M. Sheldrick, *Acta Crystallogr.* **2008**, *A64*, 112.